

Anisotropic scaling features and complexity in magnetospheric-cusp: a case study

E. Yordanova^{1,2}, J. Bergman^{3,1}, G. Consolini⁴, M. Kretzschmar⁴, M. Materassi^{5,1}, B. Popielawska¹, M. Roca-Sogorb⁴, K. Stasiewicz³, and A. W. Wernik¹

¹Space Research Center, Polish Academy of Sciences, Warsaw, Poland

²Space Research Institute, Bulgarian Academy of Sciences, Sofia, Bulgaria

³Swedish Institute of Space Physics, Uppsala, Sweden

⁴Istituto di Fisica dello Spazio Interplanetario, INAF, Roma, Italy

⁵Istituto di Fisica dei Sistemi Complessi, CNR, Firenze, Italy

Received: 2 May 2005 – Revised: 5 July 2005 – Accepted: 17 August 2005 – Published: 14 September 2005

Part of Special Issue “Nonlinear and multiscale phenomena in space plasmas”

Abstract. Magnetospheric cusps are high-latitude regions characterized by a highly turbulent plasma, playing a special role in the solar wind-magnetosphere interaction. Here, using POLAR satellite magnetic field vector measurements we investigate the anisotropic scaling features of the magnetic field fluctuations in the northern cusp region. Our results seem to support the hypothesis of a 2D-MHD turbulent scenario which is consequence of a strong background magnetic field. The observed turbulent fluctuations reveal a high degree of complexity, which might be due to the interplay of many competing scales. A discussion of our findings in connection with the complex scenario proposed by Chang et al. (2004) is provided.

1 Introduction

The interaction between the supersonic solar wind and the Earth's magnetosphere is one of the central topics of the space plasma physics studies. After more than 30 years studies the overall nature of the solar wind-magnetosphere coupling is quite well understood with respect to large scale processes. However, the knowledge of small scale phenomena and processes requires still further studies, especially related with plasma transport across turbulent boundary regions. In this framework, the characterization of the turbulence in these boundary regions plays a central role.

Among the various magnetospheric boundary structures the two singularities, called “polar cusps”, and located in correspondence with the North and the South magnetic poles, are of significant importance for the solar wind-terrestrial coupling. As a matter of fact, the topology of the background magnetic field in such regions is important for the transfer

of mass, energy and momentum through the magnetosphere. Cusp location, shape and properties are mainly controlled by the direction of the Interplanetary Magnetic Field (IMF), the tilt of the Earth's magnetic dipole axis, and the solar wind plasma parameters (dynamic pressure, etc.) (Popielawska and Gustafsson, 2003; Russell, 2000; Zhou et al., 2000).

The boundary between the magnetopause and the cusp is characterized by strong electric and magnetic field turbulence (Gurnett et al., 1979). After Hawkeye 1 observations (Gurnett and Frank, 1978), many other space missions have done wide range frequency measurements of the plasma waves in this region (Fairfield and Hones, 1978; Pickett et al., 1999, 2002; Blecki et al., 1999, 2003). Recently, CLUSTER (the first multisatellite mission) provided high-resolution magnetic field measurements of waves at the high-altitude cusp in the ion cyclotron range (Nykyri et al., 2004), that clearly show a correlation between waves and plasma flow. In detail, waves with characteristic amplitudes $2\div 5$ nT and frequencies near the local ion-cyclotron frequency were observed in cusp regions with strong plasma flow. In cusp regions with stagnant plasma flow, the observed waves have a small amplitude (<1 nT). However, no clear generation mechanism of these waves was recognized.

A recent study (Sundkvist et al., 2005), based on CLUSTER measurements, investigates waves near the proton cyclotron frequency in the high-latitude cusp for northward IMF conditions. Using all four spacecraft simultaneously, anisotropy in the characteristic length scales was found along and across the magnetic field. The estimated wavelength perpendicular to the ambient magnetic field is of the order of a few proton gyroradii or less. The wavelength parallel to the magnetic field is at least a few times larger or more. Their observations suggest that waves below the proton cyclotron frequency are kinetic Alfvén waves, while waves above this frequency are mainly ion cyclotron waves. The existence of

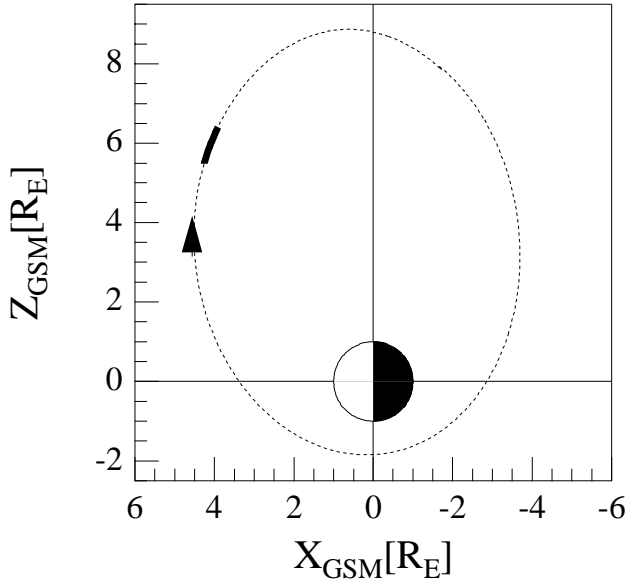


Fig. 1. The POLAR trajectory on 11 April 1997 in the XZ plane of GSM reference system. The solid black segment refers to the time interval from 12:00 UT to 13:00 UT here considered.

plasma density inhomogeneities in the range of scales similar to the wave lengths together with a finite amplitude wave field seem to point toward a crucial role of nonlinearities governing low frequency waves in the cusp.

As already mentioned, the magnetic field in the magnetosheath and in the cusp has a very complex topology, resulting in a “Turbulent Boundary Layer” (TBL) (Savin et al., 1998). TBL is found to be a permanent feature (Klimov et al., 1997; Savin et al., 2002a), and is characterized by transient, highly variable, flows of heated magnetosheath plasma (Savin et al., 2002b,c), an irregular magnetic field, and strong plasma waves (Khotyaintsev et al., 2004). The irregular magnetic field can tentatively be associated with strong (weak) magnetic field structures where magnetic force (plasma pressure) is predominant. Furthermore, evidences of a transition from a turbulent regime to a more laminar one in the deeper cusp (Pedersen et al., 2000) have been found.

In a recent paper, Yordanova et al. (2004) investigated the intermittency features of the magnetic field turbulence in the magnetospheric cusp region, as far as the total magnetic intensity “scalar” turbulence is concerned. Their results suggest that the turbulence properties strongly depend on the IMF conditions. The observed cusp turbulence has been compared with models, originally introduced to describe fluid turbulence. It has been shown that during northward IMF conditions the turbulence intermittency is consistent with the p -model scenario for fully developed turbulence (Meneveau and Sreenivasan, 1987). For such a case of northward IMF, Taylor and Cargill (2002) discussed the formation of a highly turbulent, albeit thin, boundary layer as a result of interaction of the fast magnetosonic magnetosheath flow with the magnetopause indentation at the cusp. However,

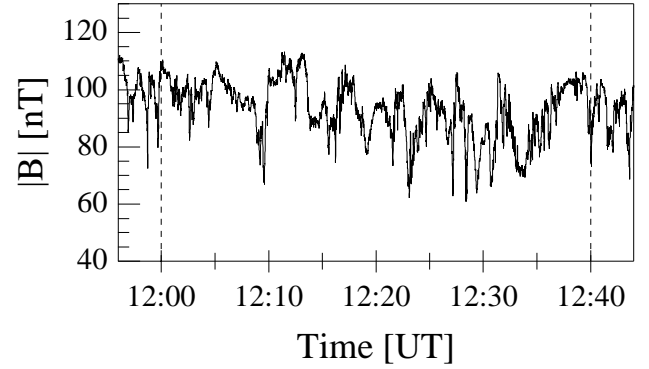


Fig. 2. The actual magnetic field magnitude as observed by POLAR satellite for the selected period. Vertical dashed lines delimit the selected time interval from 12:00 UT to 12:40 UT.

under northward IMF another scenario, involving reconnection outflow of a different character, might be also possible. For southward IMF conditions, a more proper turbulence scenario seem to be that represented by a non-fully developed Kolmogorov-like fluid turbulence model, suggesting that the observed turbulence is dominated by flow eddies (Tu et al., 1996).

In this paper we present a case study of the anisotropy features of the magnetic field fluctuations in the magnetospheric high-altitude polar cusp, as revealed by the spectral and scaling properties of the magnetic field fluctuations measured by the POLAR satellite. We investigate the turbulent features in the polar cusp by means of novel approaches based on structure functions analysis and on the study of the probability distribution functions (PDFs) of the magnetic field fluctuations at different timescales. The results of our analysis are discussed in the framework of a 2D-MHD scenario, recently proposed by Chang et al. (2004), and involving complexity and intermittent turbulence arising from the evolution of coherent magnetic and plasma structures.

2 Data description

Data used in this work refer to 3D magnetic field measurements from the POLAR satellite (Russell et al., 1995) on 11 April 1997, 12:00–12:40 UT, during which the POLAR satellite crosses the northern cusp. We concentrate our attention to the cusp region in the magnetic latitude range from $\sim 61^\circ$ to $\sim 67^\circ$ ($13:40 \div 14:13$ MLT). The satellite passage through the cusp proper was followed by the crossing of the turbulent boundary layer with magnetic bubbles, which has been analysed by Stasiewicz et al. (2001). Assuming a one hour transit time, the IMF conditions as observed by the WIND satellite at a distance of $\sim 230 R_E$ for the period here investigated, were the following (data comes from NSSDC/CDA website): IMF direction is northward, B_{IMF} components in GSM reference system is $[-6, -7, 20]$ nT, solar wind velocity is $|v| \sim 480$ km/s, proton density $N_p \sim 10 \text{ cm}^{-3}$, and proton temperature $T_p \sim 2 \div 3$ eV. In Fig. 1 the trajectory of the

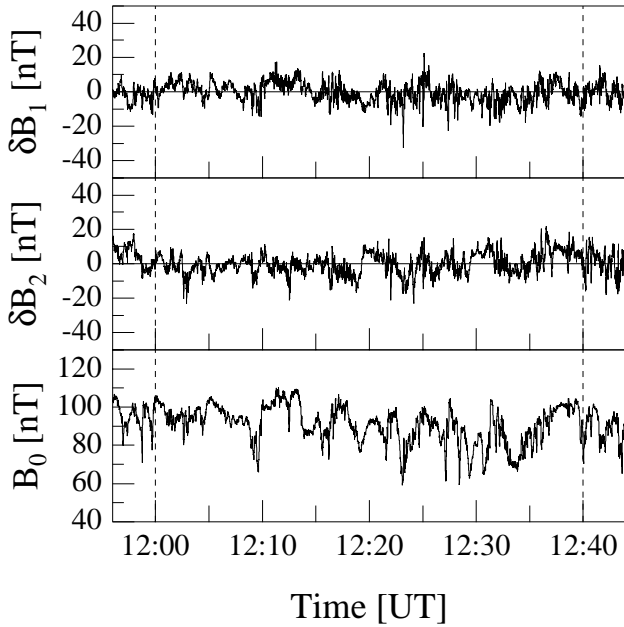


Fig. 3. The magnetic field components in the FAC system. Vertical dashed lines delimit the selected time interval from 12:00 UT to 12:40 UT.

POLAR satellite for the selected time period within the cusp is shown. Figure 2 shows the total magnetic field sampled at the rate of 8.33 s^{-1} .

From the data presented in Fig. 2 it is possible to argue that the magnetic field in such a region is characterized by an intense average magnetic field. The average magnetic field is $B \sim 90 \text{ nT}$ and the fluctuating part is $\delta B \sim 10 \text{ nT}$ ($\delta B/B \sim 0.1$). Due to the large scale magnetic field topology in such a region, this simple observation suggests that the nature of the turbulent fluctuations could be better described in the framework of reduced 2D-MHD turbulence (Shebalin et al., 1983; Cho et al., 2002). Furthermore, the features of the observed turbulent fluctuations are expected to be anisotropic in the parallel and perpendicular orientations with respect to the average, background, magnetic field direction.

To investigate the anisotropy features of the magnetic field fluctuations we have first projected the magnetic field components into a Field Aligned Coordinate (FAC) system, where the third-axis of the new reference system is chosen parallel to the mean magnetic field direction, i.e.:

$$(B_{xy}, B_z, B_{56}) \longrightarrow (\delta B_1, \delta B_2, B_0) \quad (1)$$

Here, (B_{xy}, B_z, B_{56}) are the magnetic field components measured in the satellite spin plane reference system (B_{xy} lies in the spin plane and is parallel to antisunward direction, B_z lies in the spin plane and points northward, B_{56} is along the spin axis and is duskward), and $(\delta B_1, \delta B_2, B_0)$ are the new reference frame components. In detail, B_0 is chosen parallel to the average, background, magnetic field direction and pointing toward the geomagnetic pole, and δB_i ($i=1, 2$) in a plane orthogonal to the average, background, magnetic field

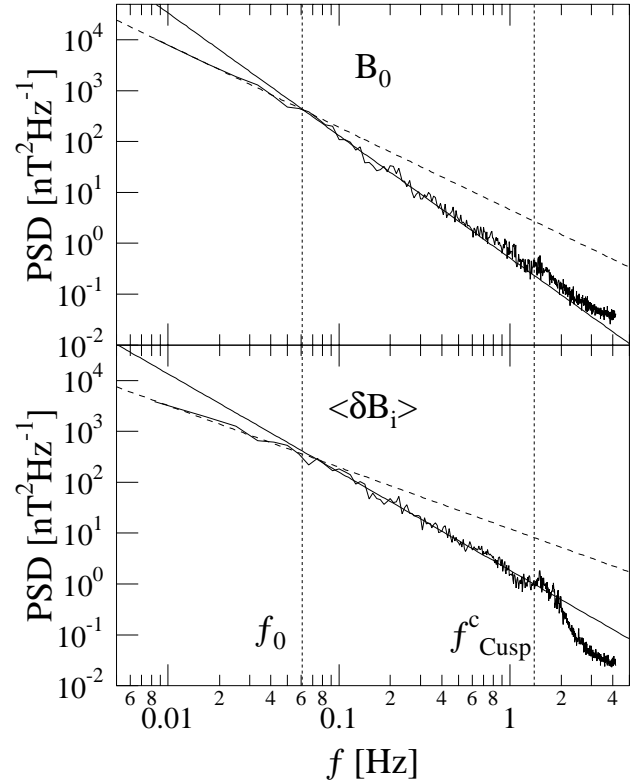


Fig. 4. The Power Spectral Density of the magnetic field components in the new reference frame. In detail, upper panel refers to PSD of the main B_0 component, while the lower panel reports the average PSD for the two perpendicular components δB_i . Solid and dashed lines are power law best fits. The two vertical lines refer to low-frequency spectral break (f_0) and the estimated cusp ion-cyclotron frequency (f_{Cusp}^c).

direction without a preferential direction. The new reference system has been chosen to be right-handed. Furthermore, perpendicular magnetic field components (δB_i with $i=1$ and 2) have been detrended for long timescale trend. Figure 3 shows the three components in the new reference system. In the new reference system we get $\langle B_0 \rangle = [91 \pm 9] \text{ nT}$, and $\langle \delta B_{1,2} \rangle = [0 \pm 6] \text{ nT}$.

3 Data analysis and results

In order to investigate the features of the magnetic field fluctuations in the parallel and perpendicular directions to the mean magnetic field orientation, we start our analysis by discussing the power spectral features in the two directions.

Figure 4 shows the Power Spectral Density (PSD) of the magnetic field in the parallel direction (upper panel) and in the perpendicular direction (lower panel) as evaluated using the periodogram technique (window length $\sim 120 \text{ s}$). The first notable fact is that both PSDs show different power-law regimes ($PSD(f) \sim f^{-\alpha}$) separated by well defined breaks, and characterized by different scaling exponents. In detail, the PSD of the main magnetic field component B_0 (upper

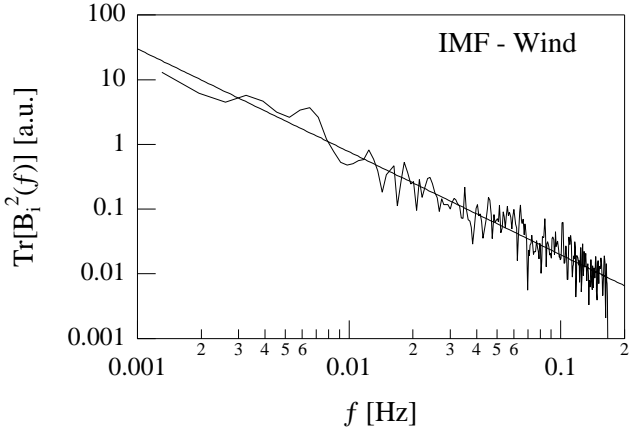


Fig. 5. The Power Spectrum of the SW magnetic field components (here reported as the trace of the PSD matrix) and observed by WIND nearly 1 hr in advance to the selected POLAR period). The solid line is a nonlinear power-law best fit characterized by an exponent $[1.59 \pm 0.03]$.

panel, Fig. 4) displays two different power-law regimes (Region I, $f < f_0$; Region II, $f > f_0$) characterized by scaling exponents $\alpha = [1.62 \pm 0.02]$ and $\alpha = [2.41 \pm 0.02]$ in Region I and II, respectively. Let us note that the Kolmogorov-like ($f^{-5/3}$) at frequencies $f < f_0$ resembles the solar wind spectral features as observed by WIND for the same period (see Fig. 5), suggesting that the long timescale axial magnetic field fluctuations are mainly driven by solar wind. Conversely, the PSD scaling features at frequencies higher than the spectral break seem to be of a different origin (Zeleniy and Milovanov, 2004), as they show $\alpha \sim 2.4$. From the average spectral properties of the perpendicular (δB_i) components (lower panel, Fig. 4) we see how this PSD shows three different regions: (i) Region I, $f < f_0$, $\alpha = [1.21 \pm 0.02]$; (ii) Region II, $f_0 < f < f_{Cusp}^c$, $\alpha = [1.93 \pm 0.02]$; (iii) Region III, $f > f_{Cusp}^c$, $\alpha \sim 5$.

The analysis of the spectral features of the magnetic field components in the parallel and perpendicular directions to the average, strong, background magnetic field clearly evidenced how the fluctuations of the magnetic field are mainly anisotropic. In order to better characterize the observed anisotropy we have investigated the scaling features of structure functions $S_q(\tau)$ of the magnetic field fluctuations using the “Extended Self-Similarity” (ESS) analysis (Benzi et al., 1993; Bershadskii and Sreenivasan, 2004). This is essentially based on the investigation of the scaling features of the q -th order structure functions $S_q(\tau)$ by studying the relative scaling of $S_q(\tau)$ with respect of a fixed p -th order structure function, i.e.:

$$S_q(\tau) \sim [S_p(\tau)]^{\eta_p(q)} \quad (2)$$

where the structure function of order q (or p) is defined according to:

$$S_q(\tau) = \langle |B_i(t + \tau) - B_i(t)|^q \rangle. \quad (3)$$

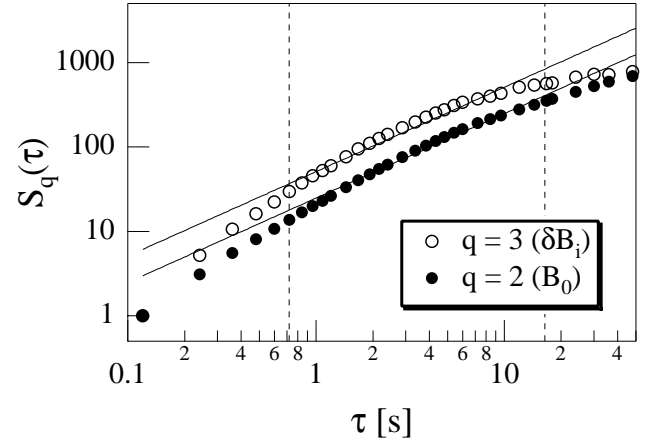


Fig. 6. The 2nd and 3rd order structure functions of the parallel (B_0) and perpendicular (δB_i) magnetic field components in the cusp region as measured by POLAR satellite. Error bars are inside symbols. The two solid lines refers to a linear dependence ($S_q(\tau) \sim \tau$). The two vertical dashed lines are respectively related to the two characteristic frequencies reported in Fig. 4 ($\sim 1/f_{Cusp}^c$ and $\sim 1/f_0$, respectively).

The “brac-kets”, $\langle \dots \rangle$, denote averaging over time, and B_i is the i -th component of the magnetic field vector. Now, in the case of scaling invariance, the q -th order generalized structure function is expected to scale as:

$$S_q(\tau) \sim \tau^{\zeta(q)} \quad (4)$$

where the scaling exponent $\zeta(q)$ is generally a convex function of the moment order q . We remark that in absence of intermittency, the scaling exponent depends linearly on the moment order q : in particular $\zeta(q) = q/m$ with $m = 3$ or 4 for fluid or MHD turbulence, respectively.

From the above considerations it follows that using the ESS, we can investigate the scaling range by plotting the q -th order structure function $S_q(\tau)$ versus the p -th order structure function, being the order p chosen so that $S_p(\tau) \sim \tau$. In this case we obtain $\eta_p(q) \equiv \zeta(q)$.

Since, empirically, the second-order scaling exponent of the parallel structure function and the third-order scaling exponent of the perpendicular structure function are very close to unity (see Fig. 6), we can apply the ESS analysis as follows:

$$\begin{cases} S_q(\tau) \sim [S_2(\tau)]^{\zeta(q)} & \longleftrightarrow B_0 \\ S_q(\tau) \sim [S_3(\tau)]^{\zeta(q)} & \longleftrightarrow \delta B_i \end{cases}, \quad (5)$$

and limit our investigation to temporal scales shorter than $1/f_0$.

Figure 7 shows the scaling exponents $\zeta(q)$ evaluated using the ESS analysis respectively for parallel and perpendicular directions. The most striking feature of the ζ scaling exponents is that while for the B_0 components these scaling indices follows a nearly linear trend (apart from a slight deviation for $q > 3$ where the statistics is strongly reduced),

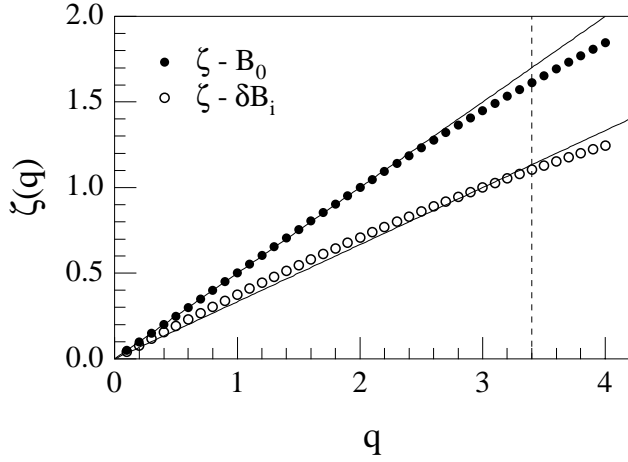


Fig. 7. The scaling exponents $\zeta(q)$ as evaluated using the ESS analysis in the case of parallel (B_0) – black dots – and perpendicular (δB_i) – white circles – directions, respectively. Error bars are inside symbols. Solid lines refer to linear dependences $\zeta(q)=q/2$ and $\zeta(q)=q/3$, respectively. The vertical dashed line refers to the limiting value q_l above which the results of ESS analysis could be not statistically valid ($q_l=\log(N)-1$, where N is the number of points of the time series here considered).

in the case of the perpendicular direction we recover a convex dependence on the moment order. This fact is confirmed by comparing the observed $\zeta(q)$ shape with a 2nd-order polynomial in the range $q \in [0, 3]$, for which we get $\partial^2 \zeta(q)/\partial q^2 = [0 \pm 0.004]$ and $\partial^2 \zeta(q)/\partial q^2 = [-0.042 \pm 0.008]$ for B_0 and δB_i components, respectively. This result suggests a quasi-monofractal behavior in the parallel direction and a multifractal (intermittent) behavior of the perpendicular fluctuations. Furthermore, the fact that for the parallel component the 2nd structure function scales as τ , indicates that fluctuations in the parallel component resemble the scaling features of the fluctuations of a random process. These differences between parallel and perpendicular scaling features again point towards an anisotropy of the observed turbulence.

Let us now investigate the PDF scaling features of fluctuations of the squared magnetic field magnitude in the parallel and perpendicular directions (Hnat et al., 2002; Chang et al., 2004). In other words, we investigate the PDF of the fluctuations of the magnetic field energy, defined as follows:

$$\begin{cases} \Delta \delta B^2 = \delta B^2(t + \tau) - \delta B^2(t) \\ \Delta B_0^2 = B_0^2(t + \tau) - B_0^2(t) \end{cases} \quad (6)$$

where $\delta B^2 = (\delta B_1^2 + \delta B_2^2)$. We may note that in the case of mono-fractal scaling features for the PDFs it is possible to recover an approximate data collapsing according to the following functional relationship:

$$P(\Delta \phi^2, \tau) \sim \tau^{-s} P(\Delta \phi^2 \tau^{-s}, \tau) \quad (7)$$

where $\phi = B_0$ or δB , and s is an appropriate scaling exponent.

Figure 8 shows the evolution for the PDFs relative to the parallel (Fig. 8a) and perpendicular (Fig. 8b) directions. The

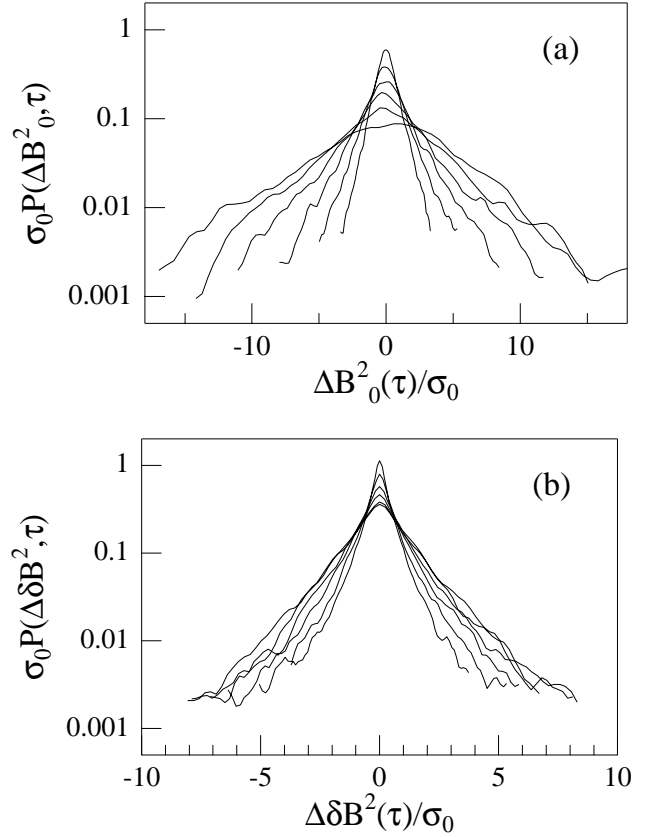


Fig. 8. The PDFs of the parallel (a) and perpendicular (b) magnetic energy fluctuations at different timescales ($\tau=6, 12, 24, 48, 96, 192\Delta t$ with Δt data sampling time lag). PDFs have been scaled for convenience using the variance σ_0 of the magnetic energy fluctuations at the timescale $\tau=6\Delta t$.

estimation of PDFs has been limited to those intervals of the variable $\Delta \phi^2$ that are statistically meaningful (i.e. we required that the occurrence frequency f_q in each bin satisfies the condition $f_q \geq 10/N_p$, where N_p is the total number of points). We may note that the PDFs are non-Gaussian and that the deviation from Gaussianity becomes more and more pronounced at shorter and shorter timescales showing a leptokurtic shape with enhanced tails. Furthermore the deviation from Gaussianity is more evident in the case of perpendicular fluctuations. This result is in agreement with the previous findings of the ESS analysis.

To evaluate the scaling exponent s of the PDFs we can investigate the scaling properties of the probability of return $P(0, \tau)$ as a function of timescale τ , that should follow a simple power law ($P(0, \tau) \sim \tau^{-s}$) (Mantegna and Stanley, 1997; Hnat et al., 2002) in the case of scaling invariant PDFs. We remark that the study of $P(0, \tau)$ is equivalent to the study of the dependency of the variance on the timescale. In Fig. 9 graphs of the $P(0, \tau)$ versus τ , for both parallel and perpendicular directions, are shown. We found that $P(0, \tau)$ follows an approximate single power-law scaling in a range from $\sim 1/f_{Cusp}^c$ to $\sim 1/f_0$, with scaling exponents $s \sim 0.56$ and $s \sim 0.4$ for parallel and perpendicular PDFs, respectively.

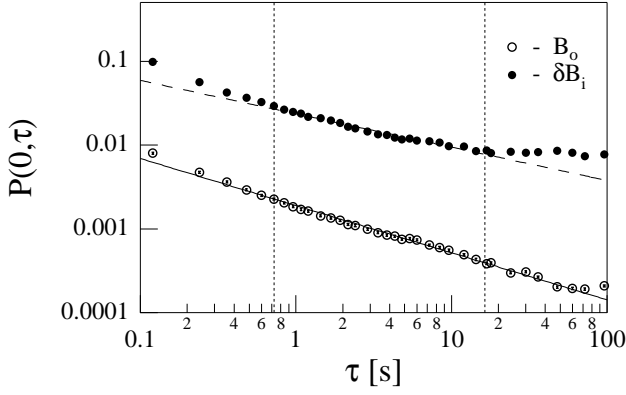


Fig. 9. The probability of return $P(0, \tau)$ for the parallel (B_0 – white circles) and perpendicular (δB_\perp – black dots) PDFs. The solid and dashed lines are power law best fits limited to the interval of timescales identified by the two vertical dotted lines at $\tau \sim 1/f_{Cusp}^c$ and $\tau \sim 1/f_0$, respectively. Error bars are inside the symbols.

In Fig. 10 we show the data collapsing relative to the PDFs of the parallel and perpendicular fluctuations using Eq. (7). Data collapsing is not good for large fluctuations ($\Delta\phi^2 \gg 0$) at long timescales in the case of perpendicular PDFs (see Fig. 10b). In other words, it actually results that the scaling relation (Eq. 7) is valid only in first approximation because the tails of the scaled PDFs do not perfectly overlap. Thus, we cannot define a universal master curve for the fluctuations following the simple scaling relationship (Eq. 7) for perpendicular PDFs. This result reflects the intrinsic multi-scaling property (intermittency) of the short timescale fluctuations, as already demonstrated by the ESS analysis. Conversely, in the case of the parallel PDFs the data collapsing is quite good (i.e. PDFs are coherent inside error bars), suggesting and supporting the quasi-monofractal character of the parallel B_0^2 fluctuations. The different behavior observed in collapsing parallel and perpendicular PDFs is confirmed by the following PDF distance measure,

$$\langle \delta_{ij}^2 \rangle = \frac{1}{N} \sum_{k=1}^N \left(\frac{f_i(x_k) - f_j(x_k)}{\delta f_i(x_k) + \delta f_j(x_k)} \right)^2 \quad (8)$$

where $f_i(x_k)$ is the value of the i -th PDF at the point x_k and $\delta f_i(x_k)$ is the associated error estimation. In detail, we found that in the case of parallel PDFs the distance of the small scale PDFs ($\tau = 6\Delta t$) from the others in the range from $\sim 1/f_{Cusp}^c$ to $\sim 1/f_0$, is nearly constant with an average value $\langle \delta_{ln}^2 \rangle \sim 0.8$, while for the perpendicular PDFs the same quantity increases from a value ~ 1 to a value > 10 in the same timescales interval. Furthermore, let us also underline that the scaled perpendicular PDF (Fig. 10b) shows a more evident non-Gaussian character with respect to the parallel scaled PDF (Fig. 10a), confirming the strong anisotropy in the fluctuations.

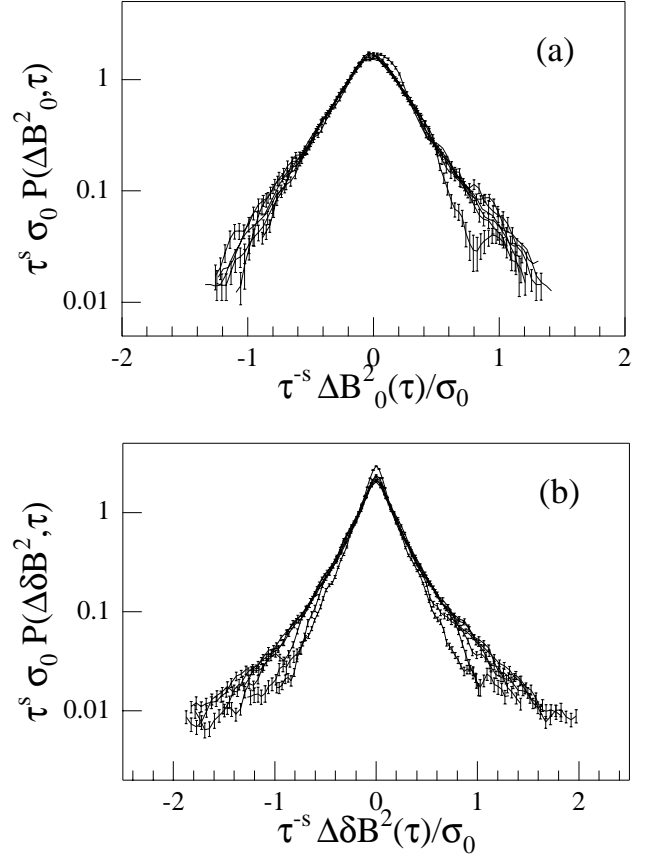


Fig. 10. The collapsing of the PDFs relative to parallel (a) and perpendicular (b) fluctuations of the PDFs reported in Fig. 8 using the expression (Eq. 7). PDFs have been scaled for convenience using the variance σ_0 of the magnetic energy fluctuations at the timescale $\tau = 6\Delta t$.

4 Discussion and conclusions

Let us start our discussion of the analysis by summarizing the results. The different techniques (spectral, ESS, and PDF shape and scaling) applied to the analysis of the fluctuations of the magnetic field in the polar cusp have clearly identified the following points:

- the PSD shows different scaling features (spectral exponents) in the parallel and perpendicular direction;
- the ESS analysis evidenced that parallel (axial) fluctuations are characterized by a nearly stochastic monofractal nature (quasi-linear dependence of the relative scaling exponents), while the perpendicular fluctuations are characterized by a strong intermittent (multi-fractal) character;
- the scaling features of the PDFs of the magnetic field energy fluctuations in the parallel and perpendicular direction confirm the more intermittent character of the perpendicular fluctuations.

All the aforementioned points indicate a strong anisotropy of the magnetic field fluctuations. Furthermore, the presence of a strong average background magnetic field suggests that the observed turbulent fluctuations could be better described in a 2D-MHD scenario (Biskamp, 2002). In this case a strong average background magnetic field would damp field-aligned fluctuations with respect to perpendicular fluctuations. The observed results seem to point toward this direction.

Recently Chang et al. (2004) proposed an alternative physical scenario for the space plasma intermittent turbulence based on a complex topology of magnetic and plasma dynamic coherent stochastic structures arising from plasma resonances and consisting of bundles of nonpropagating fluctuations. This coherent structures would appear as stochastic field-aligned flux tubes arising from the background turbulent fields, and the resulting scenario is a complex medium consisting of a hierarchy of multiscale coherent structures (see Fig. 11). This has been validated by recent 2D-MHD simulations (Wu and Chang, 2000, 2001) where the magnetic field is assumed to be represented by a scalar flux function ψ ,

$$\mathbf{B} = \mathbf{e}_z \times \nabla \psi + B_0 \mathbf{e}_z \quad (9)$$

with $B_0 = \text{constant}$ and $|\nabla \psi|^2 \ll B_0$.

Dynamic Renormalization Group (DRG) analysis, performed for simple 2D-MHD models (with or without cross-field diffusion Chang et al., 2004) has clearly shown that the Fourier transform of the correlation function of perpendicular fluctuations scales as $f^{-\alpha}$ at high frequencies, with $\alpha \sim 1.66 \div 1.88$ and $\alpha \sim 2$ for the model with or without cross-field diffusion, respectively. Furthermore, for both models, DRG analysis yields $\sim f^{-1}$ spectra at low frequencies. The -1 low-frequency spectral exponent is mean-field-like and has probably a universal character in spaceplasmas (Chang et al., 2004). Our results of the PSD of the perpendicular components δB_i seems to be very well in agreement with these predictions. As predicted by DRG analysis we, indeed, get a low-frequency region (Region I) with a nearly mean-field-like exponent ($\alpha \sim 1.2$) and a mid-frequency (MHD) region (Region II) with an exponent very near to the DRG prediction for the diffusive model ($\alpha \sim 1.9$). Furthermore, according to Matthaeus and Goldstein (1996) the low-frequency spectral exponent might be due to the superposition of uncorrelated samples of discrete coherent structures, that in the cusp assume the shape of field-aligned flux tubes.

The PSD features in the axial direction seem to have memory of the solar-wind spectral features with a nearly Kolmogorov spectrum in the low-frequency domain (Region I – $f < f_0$) and a steeper power-law region at higher frequencies (Region II – $f > f_0$). A possible explanation for this *dark-brown noise* region could be the one proposed by Zelenyĭ and Milovanov (2004). In this case the $\sim 7/3$ PSD region would be due to a rapid advection of stochastic fractal structures in respect to a rest-frame observer. This alternative interpretation is substantiated by the nearly mono-fractal character of the axial fluctuations, as evidenced by the ESS analysis, by

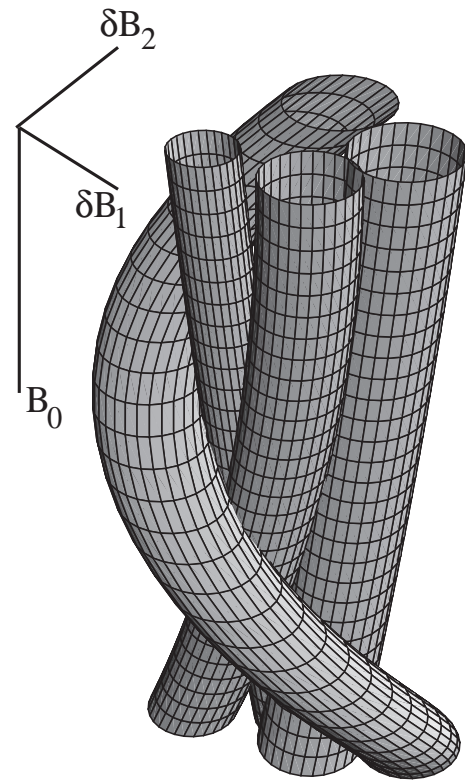


Fig. 11. A schematic drawing of a complex topology of coherent field-aligned magnetic structures.

the linear scaling of the 2nd order generalized structure function ($S_2(\tau) \sim \tau$), and by the more Gaussian shape of the PDFs of the magnetic energy fluctuations.

The scaling features of the perpendicular magnetic field and energy fluctuations exhibit intermittency, indicating a large deviation from uniformity in the distribution of scalar and/or tensor quantities. The multifractal character of perpendicular fluctuations is the signature of this dynamical intermittency. Furthermore, the scaling exponent of the probability of return $P(0, \tau)$ and the data collapsing of the perpendicular PDFs resemble the results of a similar analysis performed by Chang et al. (2004) on simulated 2D patterns. However, while Chang et al. (2004) get a $P(0, \tau)$ scaling exponent $s \sim 0.34$, we found a different value $s \sim 0.4$. The difference observed between the scaling exponents of simulated and actual data might be due to the fact that while in our case we refer to temporal fluctuations, in the case of simulated patterns the scaling exponent refers to spatial fluctuations. As a matter of fact, we remark that the conversion from spatial and temporal features in turbulent media is very crucial, being the usually adopted “Taylor’s hypothesis” not universally applicable. For example, in the case of plasma sheet turbulence it has clearly been shown that a better way to link spatial and temporal features is the “random sweeping model” (Chen and Kraichnan, 1989; Borovsky et al., 1997). In this framework, while the scale invariance is, generally, conserved, the scaling indices are expected to change.

In summary, in this work we have investigated the anisotropy of the turbulence observed in the cusp region by POLAR satellite measurements, showing how some observed scaling features of the perpendicular fluctuations in this region are in a good agreement with the scenario proposed by Chang et al. (2004) and with the results of DRG analysis on simple 2D-MHD simulations. Thus, although our results deals with a case study, they seem to point toward “an anisotropic intermittent turbulence” induced by a dynamical topological complexity that results from the nonlinear evolution of multiscale coherent structures. Let us remark that this scenario does not exclude the coexistence of propagating waves, but redefines the conventional scenario of cascading in plasma turbulence. Clearly, further work is necessary in order to confirm this scenario and to investigate the physical origin of these coherent structures.

Acknowledgements. We would like to thank T. Chang, A. V. Milovanov, and S. Y. Tam for stimulating discussions. We acknowledge L. Lepping (WIND-MFI), K. W. Ogilvie (WIND-SWE), C. T. Russell (Polar-MFE), the NASA Polar, Wind and Geotail Project, and the National Space Science Data Center (NSSDC/CDA Web) for providing data used in this work. This work is supported by the European Commission’s Human Potential Programme under contract HPRN-CT-2001-00314, “Turbulent Boundary Layers in Geospace Plasmas”.

Edited by: A. S. Sharma

Reviewed by: two referees

References

- Benzi, R., Ciliberto, S., Tripiccion, R., et al.: Extended self-similarity in turbulent flows, *Phys. Rev. E*, 48, R29–R32, 1993.
- Bershadskii, A. and Sreenivasan, K. R.: Intermittency and the passive nature of the magnitude of the magnetic field, *Phys. Rev. Lett.*, 93, 064501, 2004.
- Biskamp, D.: Response to “Comment on On two-dimensional magnetohydrodynamic turbulence”, *Phys. Plasmas*, 9, 1486–1487, 2002.
- Blecki, J., Kossacki, K., Wronowski, R., et al.: Low frequency plasma waves observed in the outer polar cusp, *Adv. Space Res.*, 23, 1765–1768, 1999.
- Blecki, J., Savin, S., Rothkaehl, H., et al.: The role of wave-particle interactions in the dynamics of plasma in the polar cusp, *Cosmic Res.*, 41, 332–339, 2003.
- Borovsky, J.E., Elphic, R. C., Funsten, H. O., et al.: The Earth’s plasma sheet as a laboratory for flow turbulence in high- β MHD, *J. Plasma Phys.*, 57, 1–34, 1997.
- Chang, T., Tam, S. W. Y., and Wu, C. C.: Complexity induced anisotropic bimodal intermittent turbulence in space plasmas, *Phys. Plasma*, 11, 1287–1299, 2004.
- Chen, S. and Kraichnan, R. H.: Sweeping decorrelation in isotropic turbulence, *Phys. Fluids A*, 1, 2019–2024, 1989.
- Cho, J., Lazarian, A., and Vishniac, E. T.: MHD turbulence: Scaling laws and astrophysical implications, arXiv:astr-ph/0205286v1, 2002.
- Fairfield, D. H. and Hones Jr., E. W.: IMF 6 measurements in the distant polar cusp during substorms, *J. Geophys. Res.*, 83, 4273–4287, 1978.
- Gurnett, D. A. and Frank, L. A.: Plasma waves in the polar cusp: observations from Hawkeye 1, *J. Geophys. Res.*, 83, 1447–1462, 1978.
- Gurnett, D. A., Anderson, R. R., Tsurutani, B. T., et al.: Plasma waves turbulence at the magnetopause: observations from ISEE 1 and 2, *J. Geophys. Res.*, 84, 7043–7058, 1979.
- Hnat, B., Chapman, S. C., Rowlands, G., et al.: Finite size scaling in the solar wind magnetic field energy density as seen by WIND, *Geophys. Res. Lett.*, 26, doi:10.1029/2001GL014587, 2002.
- Khotyaintsev, Y., Vaivads, A., Ogawa, Y., et al.: Cluster observations of high-frequency waves in the exterior cusp, *Ann. Geophys.*, 22, 2403–2411, 2004, **SRef-ID: 1432-0576/ag/2004-22-2403**.
- Klimov, S., Romanov, S., Amata, E., et al.: ASP1 experiment: measurements of fields and waves on board the INTERBALL spacecraft, *Ann. Geophys.*, 15, 514–527, 1997, **SRef-ID: 1432-0576/ag/1997-15-514**.
- Mantegna, R. and Stanley, H. E.: Physics investigation of financial markets, in: *The Physics of Complex Systems*, edited by: Malmace, F. and Stanley, H. E., IOP Press, Amsterdam, 473–489, 1997.
- Matthaeus, W. H. and Goldstein, M. L.: Low-frequency $1/f$ noise in the interplanetary magnetic field, *Phys. Rev. Lett.*, 57, 495–498, 1996.
- Meneveau, C. and Sreenivasan, K. R.: Simple multifractal cascade model of the developed turbulence, *Phys. Rev. Lett.*, 59, 1424–1427, 1987.
- Nykyri, K., Cargill, P.J., Lucek, E., et al.: CLUSTER observations of magnetic field fluctuations in the high-altitude cusp, *Ann. Geophys.*, 22, 2413–2429, 2004, **SRef-ID: 1432-0576/ag/2004-22-2413**.
- Pedersen, A., Faelthammer, C.-G., Maynard, N., et al.: Turbulent structures in the outer cusp, in: *CLUSTER-II workshop: Multiscale/multipoint plasma measurements*, edited by: Harris, R. A., ESA SP-449, 291–294, ESA Publ. Div., Noordwijk, 2000.
- Pickett, J. S., Menietti, J.D., Dowell, J.H., et al.: POLAR spacecraft observations of the turbulent outer cusp/magnetopause boundary layer of the Earth, *Nonlin. Processes Geophys.*, 6, 195–204, 1999, **SRef-ID: 1607-7946/npg/1999-6-195**.
- Pickett, J. S., Menietti, J.D., Hospodarsky, G.B., et al.: Analysis of the turbulence observed in the outer cusp turbulent boundary layer, *Adv. Space Res.*, 30, 2809–2814, 2002.
- Popielawska, B. and Gustafsson, G.: The distant cusp and the surrounding magnetopause: A view in snapshots from POLAR, *Adv. Space Res.*, 31, 1353–1362, 2003.
- Russell, C. T., Snare, R. C., Means, J. D., et al.: The GGS/POLAR magnetic field investigations, *Space Sci. Rev.*, 71, 563–582, 1995.
- Russell, C. T.: Polar eyes the cusp, in: *CLUSTER-II workshop: Multiscale/multipoint plasma measurements*, edited by: Harris, R. A., ESA SP-449, 47–55, ESA Publ. Div., Noordwijk, 2000.
- Sundkvist, D., Vaivads, A., Andr’e, M., et al.: Multi-spacecraft determination of wave characteristics near the proton gyrofrequency in high-altitude cusp, *Ann. Geophys.*, 23, 983–995, 2005, **SRef-ID: 1432-0576/ag/2005-23-983**.
- Savin, S., Borodkova, N.L., Budnik, E. Yu., et al.: Interball tail probe measurements in outer cusp and boundary layers, in: *Geospace Mass and Energy Flow: results from the International Solar-Terrestrial Physics Program*, edited by: Horwitz, J.L., Galager, D.L., and Peterson, W. K., Geophys. Monograph, 104, 25, AGU, Washington DC, 1998.

- Savin, S., Büchner, J., Consolini, G., et al.: On the properties of turbulent boundary layer over polar cusps, *Nonlin. Processes Geophys.*, 9, 443–451, 2002a, **SRef-ID: 1607-7946/npg/2002-9-443**.
- Savin, S., Zelenyi, L., Maynard, N., et al.: Multi-Spacecraft Tracing of Turbulent Boundary Layer, *Adv. Space Res.*, 30, 12, 2821–2830, 2002b.
- Savin, S., Blecki, J., Pissarenko, N., et al.: Accelerated particles from turbulent boundary layer, *Adv. Space Res.*, 30, 1723–1730, 2002c.
- Shebalin, J. V., Matthaeus, W. H., and Montgomery, D.: Anisotropy in MHD turbulence due to a mean magnetic field, *J. Plasma Phys.*, 29, 525–547, 1983.
- Stasiewicz, K., Seyler, C.E., Mozer, F.S., et al.: Magnetic bubbles and kinetic Alfvén waves in the high-latitude magnetopause boundary, *J. Geophys. Res.*, 106, 29 503–29 514, 2001.
- Taylor, M. G. G. T., and Cargill, P. J.: A magnetohydrodynamic model of plasma flow in the high altitude cusp, *J. Geophys. Res.*, 107, doi: 10.1029/2001JA900159, 2002.
- Tu, C.-Y., Marsch, E., and Rosenbauer, H.: An extended structure-function model and its application to the analysis of solar wind intermittency properties, *Ann. Geophys.*, 14, 270–285, 1996, **SRef-ID: 1432-0576/ag/1996-14-270**.
- Wu, C. C. and Chang, T.: 2D-MHD simulation of the emergence and merging of coherent structures, *Geophys. Res. Lett.*, 27, 863–866, 2000.
- Wu, C. C. and Chang, T.: Further study of the dynamics of two-dimensional MHD coherent structures – a large scale simulation, *J. Atmos. Sol. Terr. Phys.*, 63, 1447–1453, 2001.
- Yordanova, E., Grzesiak, M., Wernik, A.W., et al.: Multifractal structure of turbulence in the magnetospheric cusp, *Ann. Geophys.*, 22, 2431–2440, 2004, **SRef-ID: 1432-0576/ag/2004-22-2431**.
- Zelenyi, L. M. and Milovanov, A. V.: Fractal topology and strange kinetics: from percolation theory to problems in cosmic electrodynamics, *Phys. Uspekhi*, 47, 749–788, 2004.
- Zhou, X. W., Russell, C. T., and Le, G.: Solar wind control of the polar cusp at high altitude, *J. Geophys. Res.*, 105, 245–251, 2000.